Transactions of the Materials Research Society of Japan 29 [8] 3403-3406 (2004)

Time-Dependent Two-Dimensional Chemical Non-Equilibrium Modeling of Ar-N_2 Pulse-Modulated Induction Thermal Plasma at Atmospheric Pressure for Material Processing

Yasunori Tanaka and Tadahiro Sakuta
Department of Electrical and Electronic Engineering, Kanazawa University,
2-40-20, Kodatsuno, Kanazawa 920-8667, JAPAN
E-mail: tanaka@ee.t.kanazawa-u.ac.jp

A time-dependent two-dimensional chemical non-equilibrium model of Ar-N_2 pulse modulated induction thermal plasma (PMITP) was developed. This model takes into account thirty reactions including ionizations, dissociations and their backward reactions. Convection and diffusion effects on number density distribution of species were also considered. Thermodynamic and transport properties of thermal plasmas were calculated at each iterative calculation step using computed particle compositions at each position. Use of this model enables us to derive time variation in nitrogen atomic density distribution in the plasma torch and the reaction chamber on pulse-operation. We also predict the controllability of enthalpy and mass flow of N atom in induction thermal plasmas by the pulse-modulation of coil-current using this model.
Keywords: pulse-modulation, induction thermal plasma, chemical non-equilibrium, nitrogen atom density, enthalpy

1. INTRODUCTION

The inductively coupled thermal plasma (ICTP) at around atmospheric pressure is widely used for various materials processings, plasma waste destruction and plasma spraying because of its high temperature, high reaction activity and little contamination. However, a thermal plasma has uncontrollable high temperature, which causes a damage to substrates or products during the processings. To alleviate such a thermal problem, a 'pulse-modulated induction thermal plasma (PMITP)' system has been developed[1]–[3]. This system has a function of amplitude modulation of coil-current sustaining an induction thermal plasma. This intentional modulation may cause not only a decrease in average temperature of the induction thermal plasma, but also chemically non-equilibrium effect due to finite time of reactions. In order to investigate and predict spatial distribution of species in the PMITP, a time-dependent modelling without chemical equilibrium assumption is greatly required.

In this paper, a two-dimensional time-dependent chemical non-equilibrium (non-CE; non chemical-equilibrium) model was developed for Ar-N_2 PMITP using reaction kinetics to obtain density distribution variation. The Ar-N_2 thermal plasma is widely used for nitrification processings. In this model, the thermodynamic and transport properties such as thermal conductivity, electrical conductivity and diffusion coefficient was self-consistently calculated using non-CE composition derived at each position and time. Thirty reactions including ionization, dissociation, and their backward reactions were taken into account. Using this model, controls of enthalpy and N atom density variations were discussed.

2. PULSE-MODULATED INDUCTION THERMAL PLASMA TORCH

A conventional induction thermal plasma system needs a coil-current with a fixed amplitude to sustain an induction thermal plasma statically and steadily. In contract to this, our pulse-modulated induction thermal plasma (PMITP) system makes an amplitude modulation of the coil-current intentionally. Fig.1 indicates a general coil-current waveform for a pulse-modulated induction thermal plasma. Such a modulation of the coil-current leads a thermal plasma to be under transient state. Furthermore, non-CE effects may occur in the induction thermal plasma. Here, operation

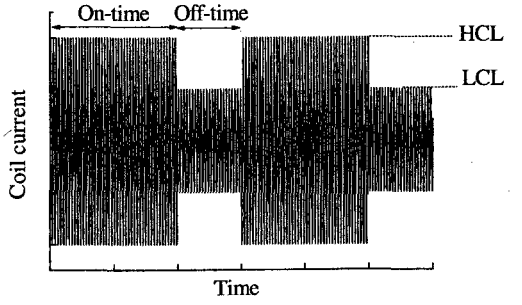

Fig. 1. Coil-current waveform of pulse-modulated induction thermal plasma.

parameters for PMITP system are defined as indicated in Fig.1; 'On-time' is the time duration when the amplitude of the current has its maximum value, 'off-time' is the time duration when the amplitude of the current has its minimum value, 'HCL' means higher current level which corresponds to current maximum value, 'LCL' is lower current level. These parameters can be set independently of one another. Another important parameter is 'shimmer current level (SCL)' which is defined as LCL/HCL.

3. MODELING OF AR-N_2 PMITP

In this calculation, the Ar-N_2 PMITP was assumed to be under the following conditions : (i) One-temperature model can be adopted. This assumption is approximately valid around plasma torch axis because of low electric field and high temperature. (ii) The plasma has an axisymetric structure. (iii) The optically thin assumption was established, and thus the effect of light absorption is negligible. (iv) There are only seven particles N_2, N_2^+, N, N^+, Ar, Ar^+ and the electron in Ar-N_2 PMITP.

4. GOVERNING EQUATION

On the basis of the assumptions described in the previous section, the PMITP behavior was simulated by simultaneously solving the time-dependent conservation equations of mass, momentum, energy and mass fraction for each species, Maxwell equation for vector potential, charge neu-

trality equation, mass balance equation, and the equation of state as follows:

Mass conservation:

$$\frac{\partial \rho}{\partial t} + \frac{\partial(\rho u)}{\partial z} + \frac{1}{r}\frac{\partial(r\rho v)}{\partial r} = 0. \quad (1)$$

Momentum conservation:

$$\frac{\partial(\rho u)}{\partial t} + \frac{\partial(u\rho u)}{\partial z} + \frac{1}{r}\frac{\partial(rv\rho u)}{\partial r} = -\frac{\partial p}{\partial z} + 2\frac{\partial}{\partial z}\left(\eta\frac{\partial u}{\partial z}\right) + \frac{1}{r}\frac{\partial}{\partial r}\left[\eta r\left(\frac{\partial u}{\partial r} + \frac{\partial v}{\partial z}\right)\right] + \mu_0\sigma\Re[\dot{E}_\theta \dot{H}_r^*], \quad (2)$$

$$\frac{\partial(\rho v)}{\partial t} + \frac{\partial(u\rho v)}{\partial z} + \frac{1}{r}\frac{\partial(rv\rho v)}{\partial r} = -\frac{\partial p}{\partial r} + \frac{\partial}{\partial z}\left[\eta\left(\frac{\partial v}{\partial z} + \frac{\partial u}{\partial r}\right)\right] + \frac{2}{r}\frac{\partial}{\partial r}\left(\eta r\frac{\partial v}{\partial r}\right) - 2\eta\frac{v}{r^2} + \mu_0\sigma\Re[\dot{E}_\theta \dot{H}_z^*]. \quad (3)$$

Energy conservation:

$$\frac{\partial(\rho h)}{\partial t} + \frac{\partial(u\rho h)}{\partial z} + \frac{1}{r}\frac{\partial(rv\rho h)}{\partial r} = \frac{\partial}{\partial z}\left(\lambda^{tr}\frac{\partial T}{\partial z}\right) + \frac{1}{r}\frac{\partial}{\partial r}\left(r\lambda^{tr}\frac{\partial T}{\partial r}\right) + \sum_j^N\left[\frac{\partial}{\partial z}\left(\rho D_j h_j\frac{\partial Y_j}{\partial z}\right) + \frac{1}{r}\frac{\partial}{\partial r}\left(r\rho D_j h_j\frac{\partial Y_j}{\partial r}\right)\right] + \sigma|\dot{E}_\theta|^2 - P_{rad} \quad (4)$$

Mass conservation of species j:

$$\frac{\partial(\rho Y_j)}{\partial t} + \frac{\partial(u\rho Y_j)}{\partial z} + \frac{1}{r}\frac{\partial(rv\rho Y_j)}{\partial r} = \frac{\partial}{\partial z}\left(\rho D_j\frac{\partial Y_j}{\partial z}\right) + \frac{1}{r}\frac{\partial}{\partial r}\left(r\rho D_j\frac{\partial Y_j}{\partial r}\right) + m_j\sum_{\ell=1}^{L}(\beta^r_{j\ell} - \beta^f_{j\ell})\left(\alpha^f_\ell\prod_{i=1}^{N} n_i^{\beta^f_{i\ell}} - \alpha^r_\ell\prod_{i=1}^{N} n_i^{\beta^r_{i\ell}}\right) \quad (5)$$

Maxwell equation by vector potential:

$$\frac{\partial^2 \dot{A}_\theta}{\partial z^2} + \frac{1}{r}\frac{\partial}{\partial r}\left(r\frac{\partial \dot{A}_\theta}{\partial r}\right) - \frac{\dot{A}_\theta}{r^2} = \bar{\imath}\mu_0\sigma\omega\dot{A}_\theta, \quad (6)$$

$$\dot{H}_z = \frac{1}{\mu_0}\frac{1}{r}\frac{\partial}{\partial r}(r\dot{A}_\theta), \quad \dot{H}_r = -\frac{1}{\mu_0}\frac{\partial \dot{A}_\theta}{\partial z}, \quad (7)$$

$$\dot{E}_\theta = -\bar{\imath}\omega\dot{A}_\theta. \quad (8)$$

Relationship between enthalpy and temperature:

$$h = \sum_j Y_j h'_j \quad (9)$$

$$h_j = \frac{1}{m_j}\left(\frac{5}{2}kT + kT^2\frac{\partial \ln Z_j}{\partial T} + \Delta H_{fj}\right). \quad (10)$$

Relation between mass density and mass fraction:

$$n_j = \frac{\rho Y_j}{m_j}. \quad (11)$$

State equation:

$$\rho = \frac{p}{\sum_j \frac{Y_j}{m_j}\kappa T}. \quad (12)$$

Quasi-neutrality of charges:

$$\frac{Y_e}{m_e} = \frac{Y_{Ar^+}}{m_{Ar^+}} + \frac{Y_{N_2^+}}{m_{N_2^+}} + \frac{Y_{N^+}}{m_{N^+}}. \quad (13)$$

Balance of mass fraction:

$$Y^T_{Ar} = Y_{Ar} + Y_{Ar^+}, \quad (14)$$

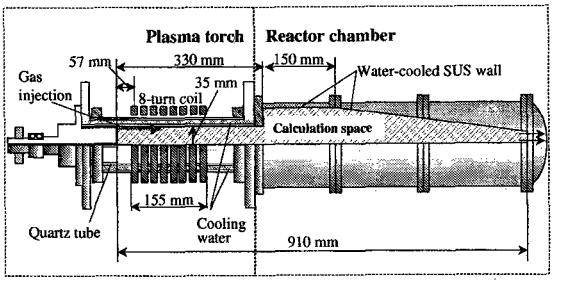

Fig. 2. Configuration of plasma torch and reaction chamber used for the present calculation.

$$Y^T_{N_2} = Y_{N_2} + Y_N + Y_{N^+} + Y_{N_2^+}. \quad (15)$$

Admixture ratio N_2 to Ar:

$$Y^T_{N_2} = \frac{m_{N_2}Q_{N_2}}{m_{Ar}Q_{Ar} + m_{N_2}Q_{N_2}}, \quad (16)$$

$$Y^T_{Ar} = 1.0 - Y^T_{N_2}. \quad (17)$$

where $\dot{A}_\theta$ is the phasor of vector potential, D_j the effective diffusion coefficient of species j, $\dot{E}_\theta$ the phasor of azimuthal component of electric field, $\dot{H}_r$ and $\dot{H}_z$ the phasors of radial and axial component of magnetic field, h the enthalpy, h_j the enthalpy of species j, $\bar{\imath}$ the complex factor ($\bar{\imath}^2=-1$), L the total number of reactions, m_j the mass of species j, N the total number of particles, n_j the number density of species j, P_{rad} the radiative loss, p the pressure, Q_{Ar} the gas flow rate of Ar gas, Q_{N_2} the gas flow rate of N_2 gas, r the radial position, t the time, T the temperature, u the axial flow velocity, v the radial flow velocity, Y_j the mass fraction of species j, Y^T_{Ar} the total mass fraction of Ar and Ar^+, $Y^T_{N_2}$ the total mass fraction of N_2, N_2^+, N and N^+, z the axial position, Z_j the internal partition function of species j, ΔH_{f_j} the standard enthalpy of formation for species j, α^f_ℓ and α^r_ℓ the reaction rates of reaction ℓ for forward and backward directions, $\beta^f_{j\ell}$ and $\beta^r_{j\ell}$ the stoichiometric numbers for species j for forward and backward reactions of the reaction ℓ, η the viscosity, κ the Boltzmann's constant, λ^{tr} the translational thermal conductivity, μ_0 the permeability of vacuum, ρ the mass density, σ the electrical conductivity, ω the angular frequency of coil current.

5. CALCULATION SPACE AND CONDITIONS

Fig.2 shows the schematic diagram of a plasma torch and a reactor chamber used in the calculation. The plasma torch has an eight-turn induction coil and water-cooled quartz tubes. The diameter of the inner quartz tube is 70 mm. The reaction chamber installed below the plasma torch is made of a water-cooled SUS304. Argon-nitrogen mixture is supplied from left-hand side in Fig.2 as a sheath gas along the inside wall of the tube. The gas flow rate is set to Ar/N_2=100/2.5 liters/min. At gas-outlet, the gas flows out freely. Temperature at each of walls is calculated considering heat transfer depending on the wall materials.

Table I summarizes reactions taken into account in the present calculation. Thirty reactions such as ionization, dissociation and their backward reactions were considered. The reaction rates of the forward reactions α^f_ℓ for reactions except 10th and 11th were estimated by Arrhenius' law as written by $\alpha^f_\ell = aT^b\exp(-c/T)$ where a, b and c are constants dependent on each reactions. The constants a, b and c are given by reference [4]. The reaction rates for the 10th

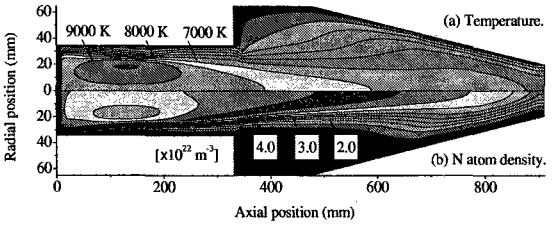

Fig. 3. Spatial distributions of temperature and nitrogen atomic density in steady state.

and 11th reactions were calculated using ionization cross sections [5].

Transport properties such as σ, λ^{th}, η and D_j were calculated by the first-order approximation of Champman-Enskog method at each of iterative calculation step at each position. A frequency of coil current is 450 kHz. Shimmer current level (SCL) was taken as a parameter. Time step was fixed at 10 μs. Pressure in the reaction chamber is atmospheric pressure 101 325 Pa. The SIMPLE algorithm after Patankar[6] was used for the calculation.

6. RESULTS AND DISCUSSIONS

6.1. Steady state

First, steady state calculation was made for Ar-N_2 ICTP. Figs.3 (a) and (b) show the spatial distribution of temperature and N atom density, respectively, in steady state for input power of 27 kW. Temperature has magnitudes above 9000 K widely in the plasma torch. Even in the reaction chamber, the temperature reaches over 6000 K. Involving such a temperature distribution, nitrogen atomic density is also distributed with a high value in the plasma torch and the reaction chamber. Generally, injecting N_2 gas is dissociated in high temperature area in the plasma torch, and then is associated in the reaction chamber. In the reaction chamber, N atom has densities above 2.0 $\times 10^{22}$ m^{-3}. At an axial position of 550 mm, N atom density reaches to its maximum above 4.0 $\times$ 10^{22} m^{-3}.

6.2. Transient state

6.2.1. Temperature

A PMITP behavior in the transient state was simulated by the amplitude modulation of the coil-current. The steady state calculation result was used as an initial value. Fig.4 shows the time evolution in the coil-current amplitude and temperature at (z [mm],r [mm])=(165,16.5) in the plasma torch. Shimmer current level is 60%. The temperature in the plasma torch is found to be modulated in conjunction with coil-current modulation. However, the temperature variation has a triangle-like waveform rather than a square-like one because of thermal inertia of the thermal plasma. In this way, 60%SCL modulation can cause temperature change between 7700 to 9700 K.

6.2.2. Nitrogen atom density

Nitrogen atom density is very important for various nitrification processing using thermal plasma. Fig.5 depicts time variation in N atom density distribution in a decaying period from 74 to 78 ms. On the other hand, Fig.6 shows time variation in N atom density distribution in a recovery period from 80 to 84 ms. During the off-period of

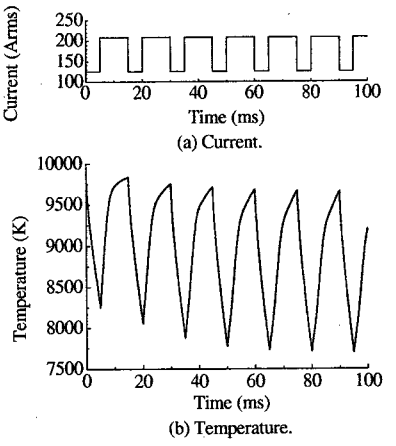

Fig. 4. Time evolution in coil-current amplitude and temperature at a position of (z [mm],r [mm])=(165,16.5) in the plasma torch. Shimmer current level is 60%.

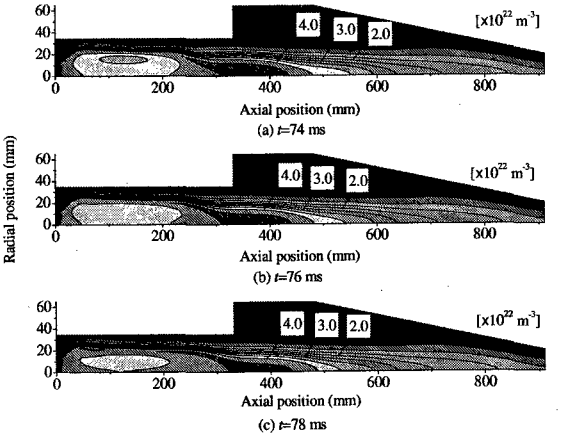

Fig. 5. Variation in N atom density in a decaying period from 74 to 78 ms after pulse modulation operation.

pulse-modulation, N atom density is produced due to recombination of N^+ and the electron in the plasma torch. In the reaction chamber, N atom density distribution slightly changes. During the on-period, N atom is ionized into N^+ in the plasma torch, while nitrogen atom produced in the plasma torch is being injected into the reaction chamber.

7. Control of enthalpy flow and mass flow of N atom

Enthalpy flow H and mass flow of N atom M_N injected from the plasma torch outlet z=370 mm in pulse-modulation operations is crucial for the thermal problem and for nitrification process to substrates. The H and M_N were calculated as follows:

$$H = \int_0^{35\ \mathrm{mm}} 2\pi\rho hurdr\Big|_{z=370\ \mathrm{mm}} \tag{18}$$

$$M_N = \int_0^{35\ \mathrm{mm}} 2\pi\rho Y_N urdr\Big|_{z=370\ \mathrm{mm}} \tag{19}$$

Figs.7 (a), (b) and (c) indicate time evolutions in coil-current amplitude, H and M_N, respectively. The time variations in H and M_N has a time-delay against pulse-modulation of the coil current. For example, a peak in H at around 85 ms is

Table I. Reactions taken into account in the present calculation.

N°	Reaction			a_ℓ	b_ℓ	c_ℓ	Reaction heat $\psi_{react\ell}$ (eV)
1	$N_2 + N_2$	→	$N + N + N_2$	4.98×10^{-9}	−1.5	113260	9.759
2	$N_2 + N$	→	$N + N + N$	2.49×10^{-8}	−1.5	113260	9.759
3	$N_2^+ + N$	→	$N_2 + N^+$	1.30×10^{-19}	0.5	0	−1.047
4	$N_2^+ + e$	→	$N + N$	2.49×10^{-8}	−1.5	0	−5.821
5	$N^+ + e + e$	→	$N + e$	2.29×10^{-20}	−4.5	0	−14.534
6	$N_2^+ + N_2 + e$	→	$N_2 + N_2$	6.07×10^{-34}	−2.5	0	−15.580
7	$N_2^+ + N + e$	→	$N_2 + N$	1.66×10^{-35}	−2.5	0	−15.580
8	$N^+ + N_2 + e$	→	$N + N_2$	6.07×10^{-34}	−2.5	0	−14.534
9	$N^+ + N + e$	→	$N + N$	1.66×10^{-35}	−2.5	0	−14.534
10	$Ar + e$	→	$Ar^+ + e + e$	-	-	-	15.760
11	$Ar + Ar$	→	$Ar^+ + e + Ar$	-	-	-	15.760
12	$N_2 + Ar$	→	$N + N + Ar$	2.49×10^{-8}	−1.5	113260	9.759
13	$N_2 + Ar^+$	→	$N + N + Ar^+$	2.49×10^{-8}	−1.5	113260	9.759
14	$N_2^+ + Ar + e$	→	$N_2 + Ar$	1.66×10^{-35}	−2.5	0	−15.580
15	$N^+ + Ar + e$	→	$N + Ar$	1.66×10^{-35}	−2.5	0	−14.534

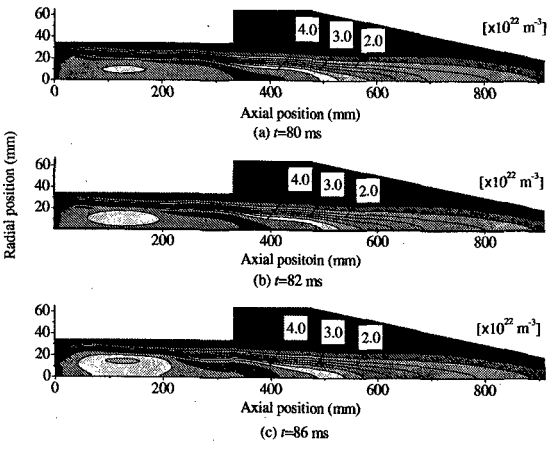

Fig. 6. Variation in N atom density in a recovering period from 80 to 84 ms after pulse modulation operation.

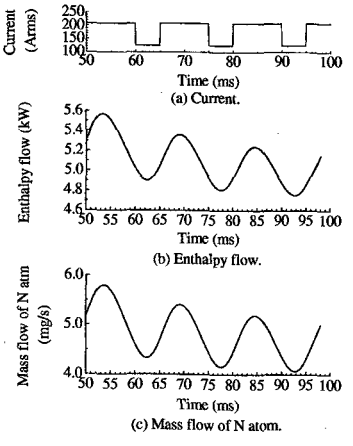

Fig. 7. Enthalpy flow and mass flow of N atom from plasma torch outlet.

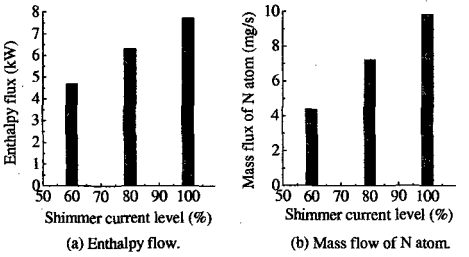

Fig. 8. Time average of total enthalpy and total mass flow of nitrogen atom from plasma torch outlet at different shimmer current levels.

considered to arise from an on-operation of 65–75 ms because it takes a delay time for the H to reach at the plasma torch outlet. Similar tendency can be found for M_N. An interesting thing in H and M_N variations is that decreasing duration in H and M_N of about 8.2 ms is longer than their increasing duration of about 6.8 ms, although the on-time and off-time are 10 ms and 5 ms, respectively.

Fig.8 shows time-averaged H and M_N from 55 to 100 ms at different shimmer current level (SCL). The time-averaged H and M_N are found to decrease with reducing SCL. This means that we can control H and M_N as a new control parameter SCL which does not exist in a conventional steady-state induction thermal plasma system.

8. CONCLUSIONS

A time-dependent two-dimensional non-CE model of Ar-N_2 PMITP was developed. In this model, thirty reactions, convection and diffusion effects were considered. Using this model, the control of enthalpy and mass flow of N atom from the plasma torch in the PMITP system can be found by the pulse modulation of the coil-current.

References

[1] T.Ishigaki et.al., *Appl. Phys. Lett.*, **71**, 3787–3789 (1997).
[2] T.Sakuta et.al., *Pure Appl. Chem.*, **71**, 1845–1852 (1999).
[3] Y.Tanaka et.al., *Plasma Sources Sci. & Tech.*, **12**, 19–26 (2003).
[4] M.G.Dunn et.al., *AIAA*, **8**, 339–345 (1970).
[5] A.V.Phelps, *J. Phys. Chem. Ref. Data*, **20**, 557–573 (1991).
[6] S.V.Patankar, "Numerical Heat Transfer and Fluid Flow", Hemisphere Publishing Corp., New York,(1980).

(Received October 8, 2003; Accepted March 12, 2004)